Energy 254 (2022) 124238

Contents lists available at ScienceDirect

Energy

journal homepage: www.elsevier.com/locate/energy

Machine-learning-based capacity prediction and construction parameter optimization for energy storage salt caverns

Jinlong Li [a], ZhuoTeng Wang [a], Shuai Zhang [a,*], Xilin Shi [b], Wenjie Xu [a], Duanyang Zhuang [a], Jia Liu [a], Qingdong Li [a], Yunmin Chen [a]

[a] MOE Key Laboratory of Soft Soils and Geoenvironmental Engineering, Center for Hypergravity Experimental and Interdisciplinary Research, Zhejiang University, Hangzhou, 310058, China
[b] State Key Laboratory of Geomechanics and Geotechnical Engineering, Institute of Rock and Soil Mechanics, Chinese Academy of Sciences, Wuhan, 430071, Hubei, China

ARTICLE INFO

Article history:
Received 22 February 2022
Received in revised form
28 April 2022
Accepted 10 May 2022
Available online 14 May 2022

Keywords:
Energy storage salt cavern
Solution mining construction
Capacity prediction
Artificial neural network
Machine learning

ABSTRACT

The construction design and control of energy storage salt caverns is the key to ensure their long-term storage capacity and operational safety. Current experimental and numerical design/optimizing methods are time-consuming and rely heavily on engineering experience. This paper proposes a machine-learning-based method for the rapid capacity prediction and construction parameter optimization of energy storage salt caverns. We propose a data generation method that uses 1253 sets of random construction parameters as input. The resulting capacity/efficiency-concerned effective volume (V) and maximum radius (r_{max}) obtained by our numerical program are the output. A back-propagation artificial neural network model for salt cavern construction prediction (BPANN-SCCP) is trained on the dataset. The cross-validated mean absolute percentage error (MAPE) of the BPANN-SCCP predicted V is 1.838%, that of the predicted r_{max} is 3.144%. This accuracy meets the engineering design requirements, and the prediction efficiency is improved by about 6×10^7 times. Using this model, a design parameter optimization method is devised to optimize 3 sets of design parameters from a million random ones. The resulting caverns are regular in shape with larger capacity ratio than 3 field caverns in Jintan Salt Cavern Gas Storage, verifying the reliability of the proposed optimization method.

1. Introduction

Global energy consumption has nearly doubled in the last three decades, increasing the need for underground energy storage [1]. Salt caverns are widely used for underground storage of energy materials [2], e.g. oil, natural gas, hydrogen or compressed air, since the host rock has very good confinement and mechanical properties. In 2020, more than 90% of the strategic oil reserves in the United States were stored in five salt caverns in Texas and Louisiana, with a total capacity of 119 million tons [3,4]. The worldwide daily gas extraction volume of the salt cavern natural gas storages is about 1.56 billion cubic meters, accounting for nearly a quarter of all gas storage reservoirs [5]. Recently, along with the promotion of carbon reduction and renewable energy [6], the studies concerning the storage of hydrogen [7], CO_2 [8] and compressed air [9,10] in salt caverns are emerging as well.

The salt cavern is constructed by solution mining [11]. Freshwater or unsaturated brine is injected into the deep salt rock formation through tubes to dissolve the salt rock and to discharge the highly saturated brines. After years of the injection-dissolution-discharge cycle, a void cavern is gradually formed, with a volume ranging from thousands to millions of cubic meters. The construction design and control of a salt cavern is very important for its safety and economic benefits. Usually the following three requirements should be satisfied.

a) Safety: the construction process should be well controlled to form a reasonable and stable form and to ensure the thickness of the salt roof [12].
b) Capacity: the salt formation should be fully utilized to obtain a larger cavern capacity in a fixed salt formation [13].
c) Efficiency: a higher construction efficiency should be achieved [13].

* Corresponding author.
E-mail address: zhangshuaiqj@zju.edu.cn (S. Zhang).

https://doi.org/10.1016/j.energy.2022.124238
0360-5442/

Abbreviations

SSCLS	Single-well Salt Cavern Leaching Simulation
BPANN-SCCP	Back Propagation Artificial-Neural-Network Salt Cavern Construction Prediction
X	Input
Y	Output
V	Effective cavern volume
r_{max}	Maximum radius of cavern
C	Cavern storage capacity
f_c	Capacity coefficient
f_e	Construction efficiency coefficient
T	Total dissolution duration
W	Safe distance between caverns
H	Cavern height
MSE	Mean Squared Error
MAPE	Mean AbsolutePercentage Error
R	Correlation coefficient

This solution mining process is a convective mass transfer process between the water and salt rock [14]. Thus, the development of the cavern boundary can be controlled by changing the boundary conditions i.e. the construction technological parameters, including the depth of the inner/outer tubes (used for injection and discharge), the depth of the blanket pad (used to protect the cavern roof), the circulation mode (direct circulation mode means injection from the inner tube, while reverse circulation mode means injection from the outer tube), the flow rate & concentration of the injected water, and the dissolution duration. During the construction of a salt cavern, these parameters need to be adjusted many times. Each adjustment is followed by a period of several months or even several years during which the operational parameters are maintained, called a “mining stage”. The cavern development is difficult to predict and control since there are many different combinations of technological parameters at different stages. Researchers have conducted extensive research on the cavern formation mechanism and prediction/design methods of salt caverns using experimental, theoretical and numerical methods as follows.

Laboratory simulation experiments are an important means to investigate the mechanism of cavern construction and to test the controlling methods. Researchers have discussed the dissolution mechanism of salt rock through laboratory dissolution experiments [15,16]. Its dependency was investigated on brine concentration, flow rate, interface angle, interface roughness, and temperature, and relevant empirical equations have been established to describe the dependency. The flow pattern and law of injection-discharge cycle have been studied through water-brine convection experiments [17,18]. Simplified flow field models with reduced dimensions have been proposed, e.g. full-cavern mass balance model [19], stratified-brine model [20] and buoyant flow model [21]. Using these simplified models, the three-dimensional turbulent flow field in the process of solution construction can be solved to predict the development of the salt cavern. Laboratory scaled-down simulation experiments have been carried out to monitor the complete solution construction [22,23]. The influence of the technological parameters on the cavern development was observed. The construction theory can be verified as well.

Researchers have developed numerical programs for cavern construction simulation, including CAVITY [24], SALT77 [25], CAVSIM3D [26], SANSMIC [27], UBRO [20], INVDIR [28], CAVITA [29], CPSLS [30], SSCLS [31], HCLS [32], TWHSMC [33], etc. They were based on the above-mentioned empirical equations of salt rock dissolution rate and simplified models of water-brine convection. SSCLS and HCLS were developed by the authors in their previous works, and the collapse and accumulation of the insoluble interlayer particles and their interaction with the dissolution of salt were considered. These programs can calculate the water-brine convection and salt dissolution using time-differentiated methods according to different geological and technological parameters, and they can simulate the dynamic cavern development. Specific construction parameters schemes can be quantitatively simulated and evaluated using these tools.

However, due to the problem of similar incongruity in the scaled-down experiments, the laboratory simulation experiments can only be qualitative, not quantitative. As for the numerical methods, they cannot give direct suggestions for the optimization of construction parameters. Operators need to simulate and adjust different parameter schemes to obtain better results. The prediction and evaluation of one design parameter scheme requires nearly half an hour of computing time using simplified numerical models or even several weeks using computational fluid dynamics models. There are so many potential combinations of different kinds of construction parameters that the design optimization using traditional methods is very time-consuming. Therefore, the discussions on design parameter optimization are limited, and actual engineering design relies heavily on the operator's design experience. As a result, there are quite a large number of irregularly shaped caverns due to improper design in China [11,32], which have not enough capacity and pose severe collapse risks.

Aiming at these problems, in this paper, we propose a machine-learning-based method, as a third option besides the physical and numerical methods, to conduct much more rapid prediction of capacity and optimization of construction design parameters for energy storage salt caverns. Machine learning methods have been widely used in engineering design [34,35], but the application to salt cavern construction prediction and optimization has not been reported. We summarize the main contributions and technique route of this study as follows.

(1) A novel data abstraction and generation method for the construction prediction of salt storages: the changing design parameters over years of construction are formatted into sets of parameters in a fixed number of stages. A random data generation rule is proposed and 1253 sets of design parameters are generated. Their resulting important evaluation indexes for the final storage service are obtained using the pre-programmed Single-well Salt Cavern Leaching Simulation (SSCLS) software [31].
(2) A successful application of machine learning methods in predicting the capacity from the construction design parameters of the energy storage salt caverns: the TRAINING, VALIDATION, and TEST datasets are created using the construction parameters as the input and the result data as the output. A back propagation artificial-neural-network salt cavern construction prediction (BPANN-SCCP) model is built and trained on the datasets until the error is reduced to a level that meets the design requirements. BPANN-SCCP can directly predict the effective cavern volume (with <2% error compared with the numerical results) and maximum radius (with 3% error) from formatted multi-stage construction parameters (then we can further calculate the capacity and efficiency coefficients based on these two results).
(3) A novel design parameter optimization scheme combining machine learning with numerical methods: a million sets of construction design parameters are randomly generated and used as input, it covers nearly all possible combinations. The corresponding results are predicted using the BPANN-SCCP

model. Optimized construction design parameters are obtained by evaluating the safety, capacity and efficiency of the predicted results. A further optimization is conducted using numerical tools to optimize the final options by taking safety concerns of cavern shapes into consideration.

2. Methodology

BPANN is a multi-layer feed-forward neural network using backpropagation algorithm. This was selected due to its strong nonlinear function fitting capability. A BPANN includes one input layer, several hidden layers, and one output layer. Each layer consists of a different number of "neurons". Each neuron passes a weighted sum of its inputs from the previous layer to the next layer until it reaches the output layer. When the output does not match with the expected output, the error is backpropagated to adjust the neuron weights and biases in each layer. This process is repeated until the error between the predicted output and the expected output is acceptable. Eventually, the neural network model can be used for prediction using similar input data. In this section, we establish a back propagation artificial neural network model for salt cavern construction prediction (BPANN-SCCP). The flow chart is shown in Fig. 1, the details will be described in the following sections.

2.1. Data generation

Establishing a reasonable database is the most critical step in establishing a predictive neural network model. All factors affecting the prediction results need to be quantified as inputs (X), and the corresponding prediction results as outputs (Y). In this paper, we simplify the geological factors by assuming that the salt layer is homogeneous and the insoluble content is 10%, then only the technological parameters are considered. Considering that the process parameters are adjustable among stages, different combinations of design parameters in different stages should all be quantified as inputs. Here we assume cases with 5 direct cycle stages. This can represent cases with fewer stages as well by inputting the same parameters in adjacent stages. The design parameters in each stage are randomly generated under the following rules:

(1) The depth of the water injection tube in the first stage is 0 m, and all the other depths are taken as values relative to this depth.
(2) The depth of the blanket pad in the last stage is 80 m, so that the heights of the final caverns are all 80 m.
(3) The depth of the water injection tube rises sequentially in each stage; each rise is not less than 10 m.
(4) The depth of the brine discharge tube in each stage is 5 m lower than the depth of the blanket pad, and these depths are always higher than the depth of the water injection tube.
(5) The depth of the blanket pad rises sequentially in each stage (the commonly used blanket material is diesel fuel, the reduction of the blanket pad requires a large amount of diesel fuel, the cost of which is high). Each of these rises is not less than 10 m.
(6) The minimum duration for each stage is 30 days and the maximum duration is 300 days. The total duration of the 5 stages is 600 days.
(7) The adjustment ranges of flow rate and concentration are small in the field, thus, the flow rate is 60 m^3/h for each stage, which is very common in the field.

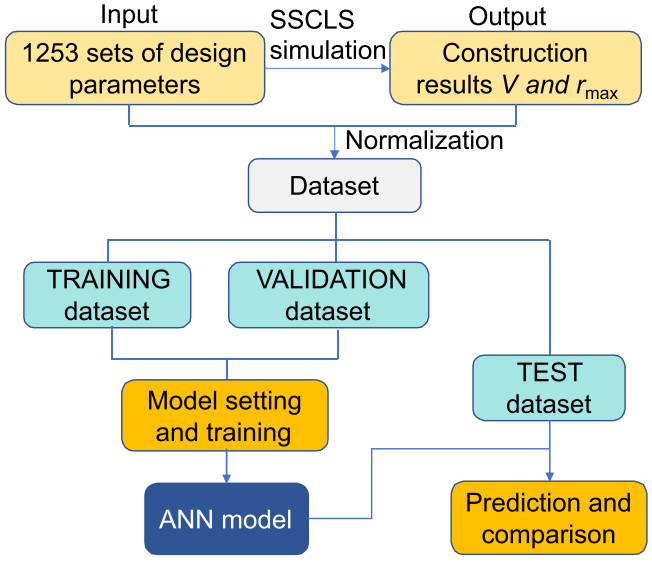

Fig. 1. Flow chart of the training and evaluation of the BPANN-SCCP model. SSCLS is our previously software, V = cavern volume, r_{max} = maximum cavern radius.

Under the above rules, we randomly generate 1253 sets of design parameters. Each set contains the water injection tube depth, brine discharge tube depth, blanket pad depth, duration, and flow rate in 5 stages. Using these parameters, we obtain 1253 simulated caverns (Fig. 2) by our previously developed SSCLS software [31]. The effective cavern volume V and maximum radius r_{max} are exported for the calculation of the most important evaluation indexes of the storage service, including storage capacity C (usually considered equal to the effective volume), capacity coefficient f_c (the ratio of the cavern capacity to its occupied space), and construction efficiency coefficient f_e (Eq. (1), proposed by Ref. [13]). These 1253 sets of 5-stage parameters and corresponding results form our initial data set. A part of the data set is shown in Table 1. The full dataset can be found in the supplementary material.

$$C = V, f_e = \frac{C}{T}, f_c = \frac{C}{(2r_{max} + W)^2 H} \quad (1)$$

where, T is the total dissolution duration, W is the safe distance between neighboring caverns, usually two times the maximum cavern diameter (or $4r_{max}$) in China [3], H is the cavern height.

2.2. Data processing

Among the previously mentioned technological parameters, the flow rate is a constant and does not need to be included in the TRAINING data set. The depth of the outer tube depends on the depth of the blanket pad, it is not an independent variable and hence does not need to be included as well. Therefore, the final input data only includes 15 items, i.e. the inner tube depth, blanket pad depth, and the duration of the 5 stages. C, f_e and f_c are dependent on V and r_{max} as per Eq. (1). Thus, the output of the data set used for training only includes two items: V and r_{max}. To improve the convergence speed and accuracy of the model, the input and output data are normalized before training. The data values in each column of the dataset are mapped to the interval [0,1]. The prediction results will be inversely normalized to the original value interval as well.

After normalization, we divide the data into three sets. 80% of the data is taken as the TRAINING set to train the model, 10% of the

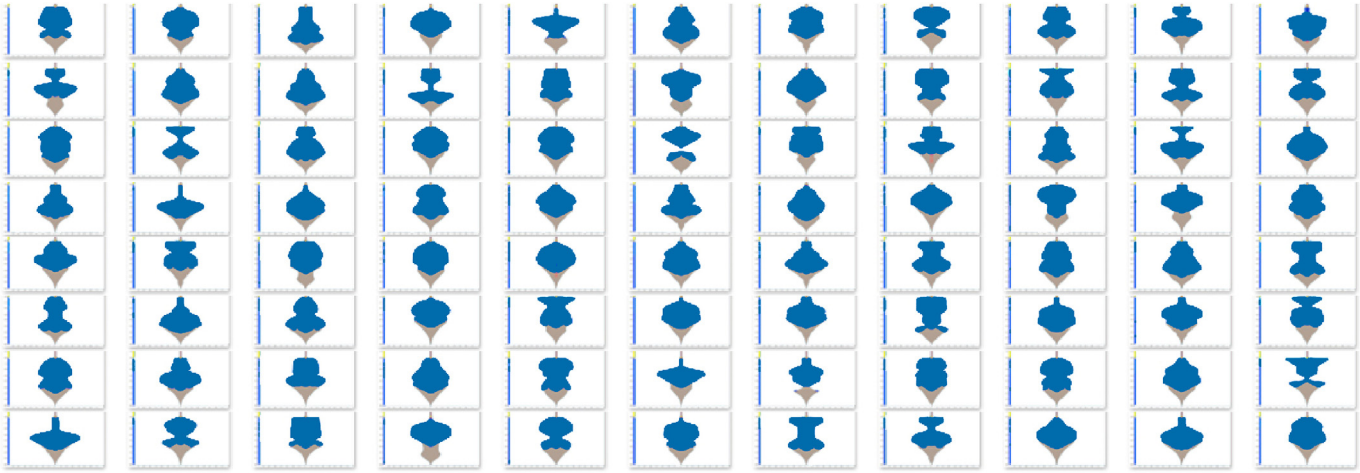

Fig. 2. A part (88) of the 1253 caverns simulated using SSCLS software [31].

Table 1
Data examples of the input design parameters and their corresponding output results.

Input							Output			
Stage 1					…	Stage 5				
Water injection depth/m	Brine discharge depth/m	Blanket pad depth/m	Dissolution duration/day	Flow rate /m^3/h	…	…	*V*/*C* /m^3	r_{max}/m	f_c	f_e /m^3/day
0	20	25	41	60	…	…	86,370	32.90	0.028	143.95
0	9	14	23	60	…	…	80,779	27.72	0.037	134.63
0	19	24	59	60	…	…	75,137	31.99	0.025	125.23
0	25	30	36	60	…	…	79,406	28.45	0.034	132.34
	…									
0	16	21	52	60	…	…	76,299	27.28	0.036	127.16

data is taken as the VALIDATION set to help prevent overfitting, and the remaining 10% of the data is taken as the TEST set to evaluate the performance of the model.

2.3. Model setting and training

The topology and the training hyperparameters of the BPANN-SCCP model are optimized through training. The topology of the final optimized model consists of an input layer, 3 hidden layers, and an output layer, as shown in Fig. 3. The input layer consists of 15 neurons corresponding to the 15 inputs (inner tube depth, blanket pad depth, and duration of 5 stages). The 3 hidden layers are fully connected, and the number of neurons in each layer is 512. The output layer consists of 2 neurons corresponding to *V* and r_{max}. The hidden layer uses the "ReLU" function [36] as the activation function, which introduces a nonlinear factor to the neural network and makes it more capable of mapping nonlinear functions.

The hyperparameters used for model training, including loss, metric, optimizer, epoch, batch size, callback, and initializer are listed in Table 2. Among them, considering that the learning rate of the neural network needs to be reduced as the model gradually converges to prevent oscillations, the model uses the "ReduceLROnPlateau" function [37] as the callback function to update the learning rate of the model automatically. The detailed parameters are set as follows: monitor = val_loss, factor = 0.2, patience = 5, min_lr = 0.001.

Fig. 4 shows the change of MSE with epoch for the TRAINING and VALIDATION data sets. At around 100 epochs, the MSE of the TRAINING set is stable at around 0.0002. The stable value of the MSE on the VALIDATION data set is higher than 0.0030, indicating the model is overfitting. This could be fixed by introducing more data, but since a MSE of 0.0030 is small enough for actual cavern design, it can be said that the model is well trained.

3. Results

3.1. Prediction accuracy

The prediction accuracy of the trained BPANN-SCCP model is evaluated using the mean absolute percentage error (MAPE) and the correlation coefficient (R) [39]. The MAPE calculates the mean value of the ratio of the error (absolute value) to its true value. The R investigates the degree of linear correlation between the model output and the measured values (R = 1 means perfectly linear).

Fig. 5 shows the MAPE and R of the predicted *V* in different data sets. The prediction accuracy is high in the TRAINING set (Fig. 5a), the R and MAPE are 0.998 and 0.509%, respectively. Tose of the VALIDATION and TEST sets are slightly lower than those of the TRAINING set (Fig. 5b and c), their Rs are 0.972 and 0.962, and those of MAPEs are 2.005% and 1.689%, respectively. The accuracy of this prediction varies across different intervals of *V*. For the half data with larger *V* (the area in the black square box in Fig. 5c), the MAPEs are 0.855% and 0.724% on the VALIDATION and TEST sets, respectively, much smaller than those of the complete data set. For half of the data with smaller *V*, the prediction error is larger. This reflects that the relation is much more complicated in this range since these caverns with smaller *V* are most irregular due to inappropriate parameter design. The goal of this model is to select the parameters with larger *V*, thus the prediction accuracy with larger *V* is relatively more important. Therefore, it can be considered that the capacity

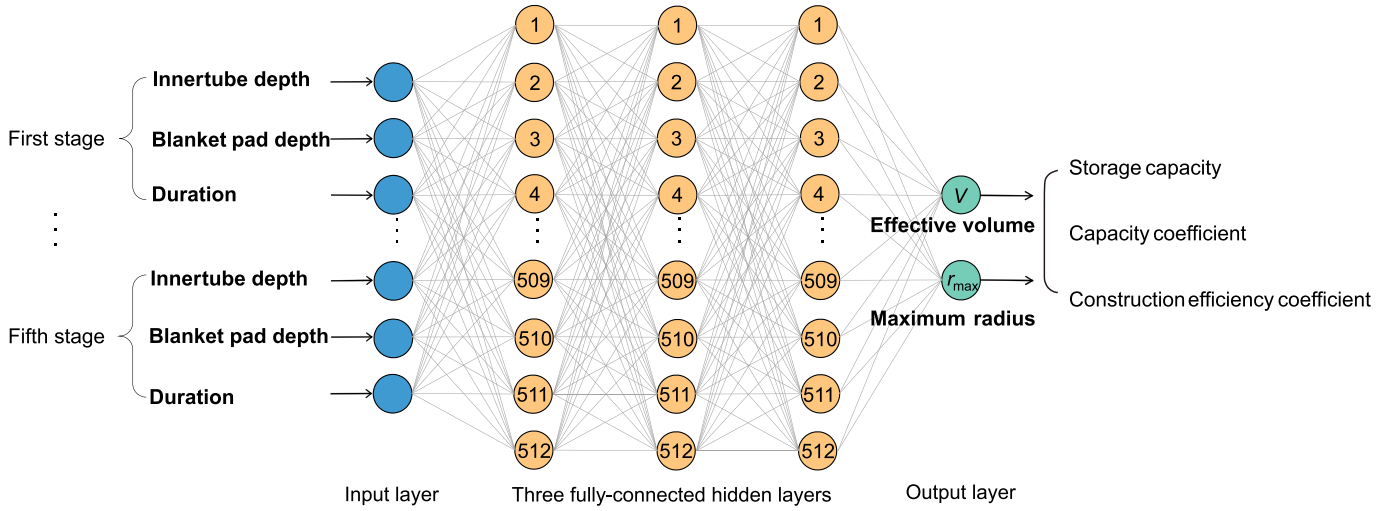

Fig. 3. Topology of the BPANN-SCCP model.

Table 2
Training hyperparameters used for model.

Hyperparameter	Setting
Loss	Mean squared error (MSE)
Metric	Mean absolute error (MAE)
Optimizer	Adam [38]
Epochs	200
Batch size	5
Callback	ReduceLROnPlateau
Initializer	Normal [37]

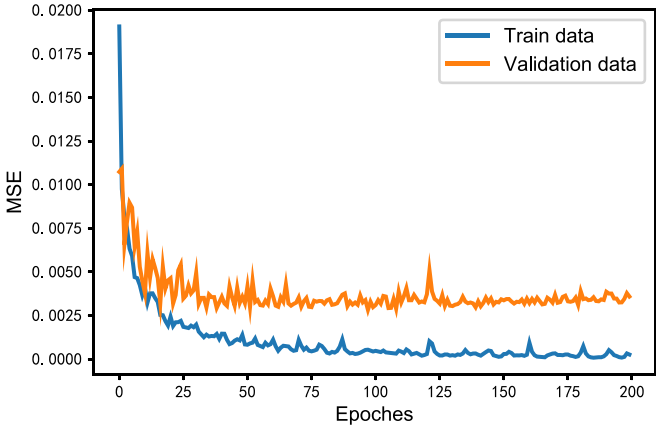

Fig. 4. Trend of MSE (Mean Square Error) of the model on the TRAINING and VALIDATION data sets.

and efficiency prediction MAPE of the model is better than 1% and can meet the requirement of prediction accuracy in actual engineering.

Fig. 6 shows the MAPEs and Rs of the predicted maximum cavern radius r_{max} in different data sets. The Rs are 0.918 and 0.892 for the VALIDATION and TEST set (Fig. 6b and c), and their MAPEs are 3.065% and 3.067%, respectively. Overall, the prediction accuracy of r_{max} is lower than that of V. However, a MAPE of 3% is still within the acceptable error range for actual engineering design and is acceptable for our goal of preliminary parameter optimization as well.

To make sure the test results are general, we conduct a 10-fold cross-validation. The data is randomly split and trained 10 times. For this validation, the average MAPE of V is 1.838% and that of r_{max} is 3.144%, as shown in Table 3. It can be said that this BPANN-SCCP model can directly predict the V and r_{max} according to the multi-stage construction parameters, and the prediction accuracy meets the actual engineering requirements, while the prediction efficiency is greatly improved by about 6×10^7 times.

3.2. Parameter optimization

In this section, the parameter optimization is discussed. As suggested in the introduction, a good parameter design should lead to a larger capacity (C), a higher capacity coefficient (f_c), and a higher efficiency coefficient (f_e). Based on the parameter rules described in Subsection 2.2, we randomly generate one million sets of parameters, and predict their corresponding results (V and r_{max}) using BPANN-SCCP, and then calculate C, f_c and f_e. As has been presented in Section 2.2, the total duration is fixed, and f_e can be represented by C. Thus, only the normalized C and f_c are calculated, summed, and ranked. 100 sets of parameters with the highest normalized C and f_c are obtained. Considering that the prediction error of the maximum radius r_{max} is larger than that of the volume V, we select 10 sets with the largest C among the selected 100 sets as the final optimized parameters. The data generation, model prediction, and ranking screening of one million sets of technological parameters take 1.53 s, 27.88 s, and 0.40 s of computing time, respectively. It means the proposed method can evaluate one set of construction parameter in less than 3×10^{-5} s (a traditional method would cost half an hour). This convincingly shows that the BPANN- SCCP method greatly improves the efficiency of the prediction and preliminary optimization of design parameters.

The current prediction cannot reflect the cavern shape, which is of great concern for stability analysis. Further manual optimization is needed to make sure the final cavern shapes are reasonable. Using the 10 parameter sets selected by BPANN- SCCP, construction simulations are carried out using SSCLS software. We manually remove those cases with a large flat top or with other unreasonable forms. Three sets of parameters are finally selected as shown in Table 4 (the outer tube depth is taken as 5 m lower than the blanket pad depth, and the flow rate is 60 m^3/h).

To further discuss the optimization results, the shapes and capacity coefficients (f_c) of the optimized caverns (A, B, C) are compared with those of 3 actual salt caverns (JT86, JT103, JT86 in

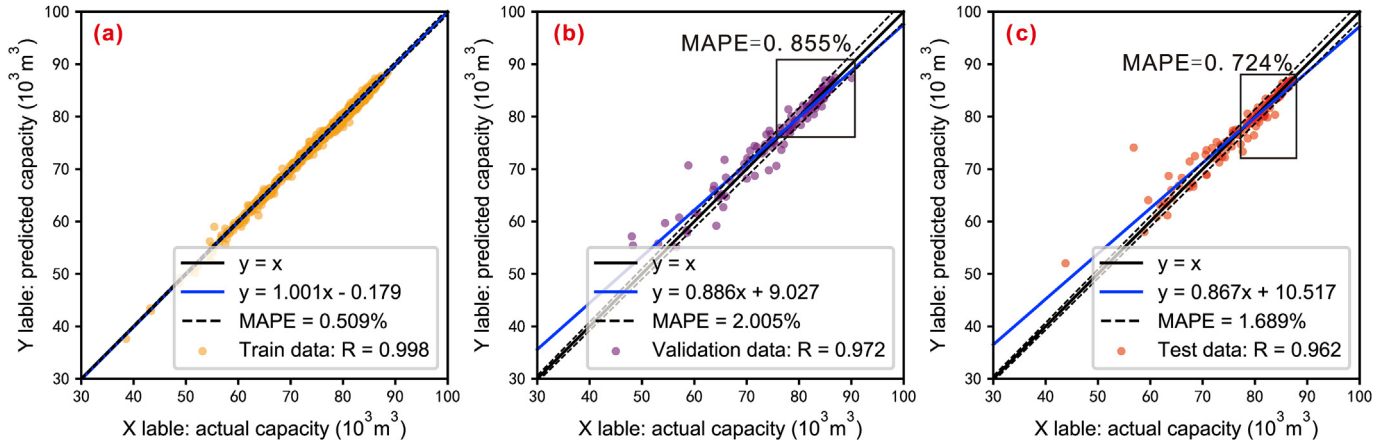

Fig. 5. Deviation between predicted V and actual V: (a) TRAINING data set, (b) VALIDATION data set and (c) TEST data set.

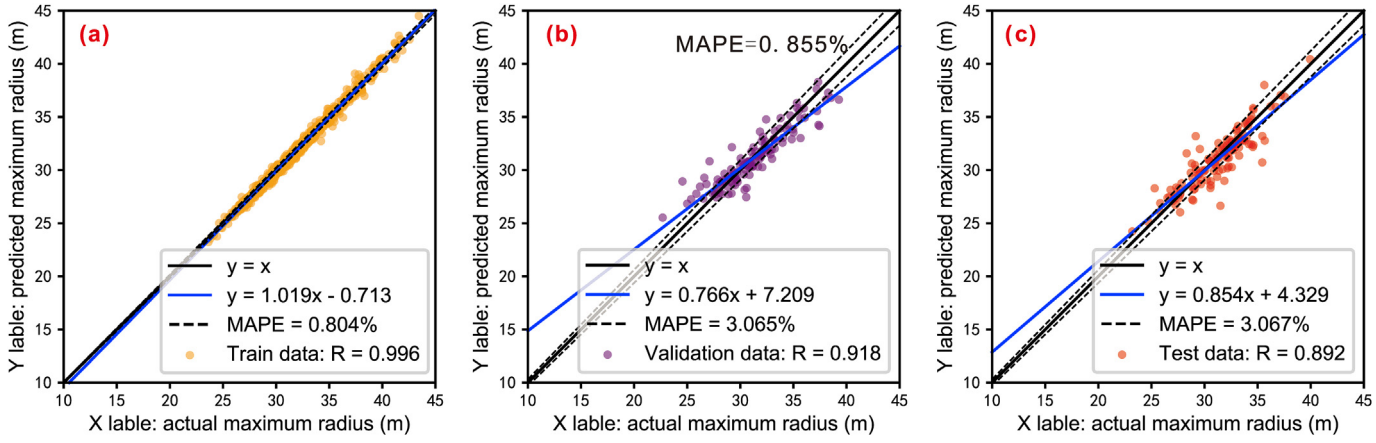

Fig. 6. Deviation between predicted r_{max} and actual r_{max}: (a) TRAINING data set, (b) VALIDATION data set and (c) TEST data set.

Table 3
MAPEs (Mean Absolute Percentage Errors) of 10-fold cross-validation.

Predicted item	MAPE			
	Maximum value	Minimum value	Mean value	Variance
V	2.042	1.672	1.838	0.017
r_{max}	3.452	2.948	3.144	0.032

Jintan Salt Cavern Gas Storage). We chose these three caverns because they are very close in capacity while their shapes and f_c values are quite different. The comparison results are shown in Fig. 7 and Fig. 8. The three caverns are larger than those of A, B, C, thus we shrink their size to facilitate the comparison in Fig. 7. Considering that the cavern capacity is highly affected by the insolubles content, a total capacity coefficient f_{tc} is calculated and

Table 4
3 sets of design parameters manually selected from the 10 sets optimized using BPANN-SCCP.

	Stage	Duration/day	Inner tube depth/m	Outer tube depth/m	Blanket pad depth/m	Flow rate/m^3/h
A	1	33	0	11	16	60
	2	164	8	45	50	60
	3	216	12	60	65	60
	4	99	46	70	75	60
	5	88	59	75	80	60
B	1	29	0	7	12	60
	2	133	8	44	49	60
	3	227	13	59	64	60
	4	122	26	69	74	60
	5	89	61	75	80	60
C	1	30	0	14	19	60
	2	100	7	45	50	60
	3	248	16	60	65	60
	4	123	42	68	73	60
	5	99	59	75	80	60

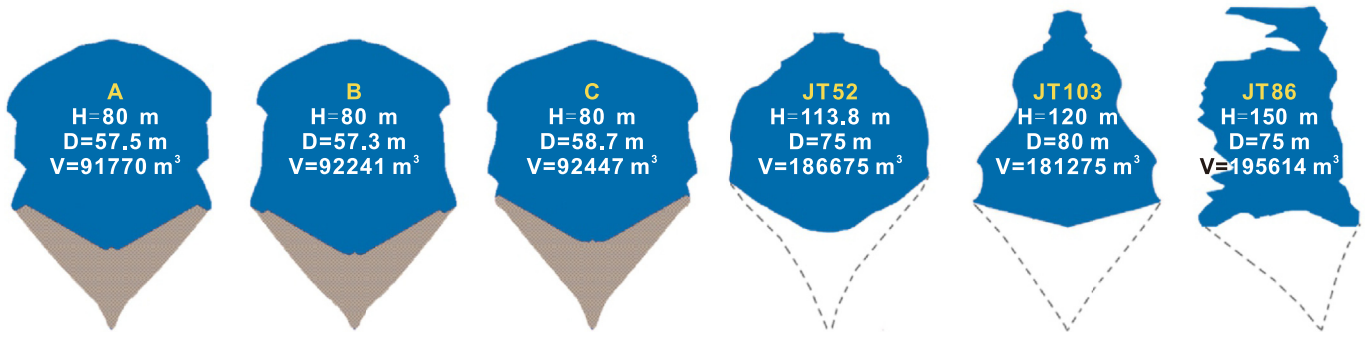

Fig. 7. Comparison of the optimized caverns (simulated using A, B, C parameters in Table 4) and the actual field caverns (JT52, JT103, JT86 in Jintan Salt Cavern Gas Storage).

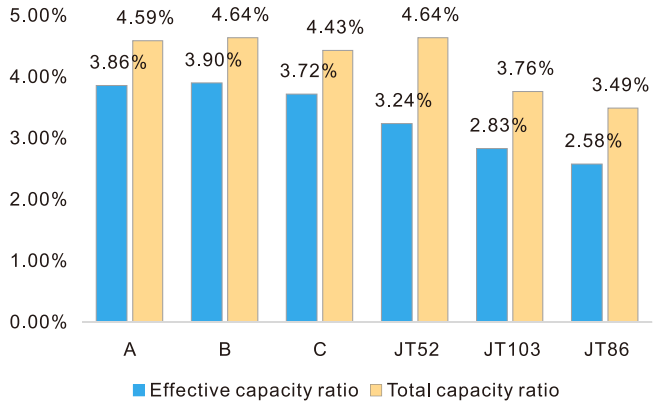

Fig. 8. Comparison of the capacity ratios of the optimized caverns (simulated using A, B, C parameters in Table 4) and the actual field caverns (JT52, JT103, JT86 in Jintan Salt Cavern Gas Storage).

compared to exclude the effect of different insoluble contents.

$$f_{tc} = \frac{f_c}{1 - f_{ins} f_{exp}} \tag{2}$$

where, f_{ins} is the insolubles content, f_{exp} is the expansion ratio of the insolubles in brines.

JT52 is a typical successfully designed cavern. It has a quite axisymmetric and regular shape and its capacity coefficients are very high, f_c is 3.24% and f_{tc} is 4.64%. As for JT103, its top half is much smaller that its bottom half, its height and maximum diameter are both larger than those of JT52, while its effective capacity is nearly the same. Thus, its capacity coefficients are much lower than those of JT52. The JT86 is an irregularly shaped cavern with a large overhanging block, resulting from insoluble interlayers probably. Its capacity coefficients are even smaller.

In comparison, our 3 optimized caverns are all regular in shape, their f_cs are about 3.72%–3.9%, higher than all of the actual caverns, as shown in Fig. 8. The f_{tc}s are about 4.43%–4.64%, higher than those of JT103 (3.76%) and JT86 (3.49%), close to that of JT52 (4.64%). It is clear that the proposed optimization method helps to achieve more regular shapes and higher capacity coefficients during the design of energy storage salt caverns.

4. Conclusions and discussion

The traditional physical or numerical simulation methods to optimize the construction design parameters of energy storage salt cavern are time-consuming and rely heavily on engineering design experience. In this paper, we propose a machine-learning-based method to help capacity prediction and parameter optimization for salt caverns. A back propagation artificial neural network-based salt cavern construction prediction (BPANN-SCCP) model is established. It takes the construction design parameters as inputs to predict the effective cavern volume (V) and maximum cavern radius (r_{max}). They are important evaluation indexes reflecting the final storage capacity and construction efficiency, as per Eq. (1). We propose and discuss a rapid parameter optimization method using the BPANN-SCCP model. The detailed works and main conclusions are as follows.

(1) We devise a data generation method for salt cavern construction prediction. 1253 sets of technological design parameters (including the depth of inner and outer tube and blanket pad, the water injection flow rate, and the duration of five construction stages) are generated using a random parameter generator. The corresponding cavern volume V and maximum cavern radius r_{max} are obtained using a previously developed Single-well Salt Cavern Leaching Simulation (SSCLS) software. The normalized inner tube depth, blanket pad depth, and duration of the five stages are used as input data, and the normalized V and r_{max} are used as output data to form the dataset required for training the neural network. This dataset is 8:1:1 split into TRAINING, VALIDATION and TEST sets for training, validation and evaluation of the network.

(2) We establish and train a 5-layered BPANN-SCCP model through topology and hyperparameter optimization. The prediction accuracy of V and r_{max} is discussed. The correlation coefficients (Rs) of V in the TRAINING, VALIDATION, and TEST sets are all higher than 0.96, and the mean absolute percentage errors (MAPEs) are lower than 2.1%. For the half data with larger V, which is more important for construction design, the MAPE is 0.724% in the TEST set. The correlation coefficient R of r_{max} in the TRAINING, VALIDATION, and TEST sets is higher than 0.89 and their MAPEs are less than 3.1%. The MAPEs of V and r_{max} on the TEST set in a 10-fold cross-validation are 1.838% and 3.144%, respectively. The prediction accuracy of V and r_{max} are high enough to meet the design requirements. The prediction efficiency is greatly improved, by about 6×10^7 times. One traditional numerical prediction requires half an hour of computing time, while one BPANN-SCCP prediction requires only about 3×10^{-5} s. It is demonstrated that the neural network is highly applicable in the nonlinear prediction of capacity and construction efficiency of energy storage salt caverns.

(3) We propose a novel design parameter optimization method for salt cavern construction. We generate one million sets of randomly generated construction parameters and predict the

resulting V and r_{max} using the BPANN-SCCP model. One hundred sets of parameters, those with the highest sum of normalized capacity and efficiency and capacity coefficients (calculated by V and r_{max}) are preliminarily selected. Considering that the prediction error of V is smaller, 10 sets of parameters with the highest capacity within these pre-selected 100 sets are selected as the final optimized parameters. The whole data generation, prediction and optimization process of 1 million sets of random parameters takes less than 30 s of computing time. The simulated caverns obtained by SSCLS using the optimized parameters are regular in shape, with larger capacity ratio compared with three actual field caverns in Jintan Salt Cavern Gas Storage.

In this paper, the dataset is generated using numerical simulation tools, and only a uniform salt layer and direct circulation construction mode are considered. In the future, more adverse geological parameters as well as variable circulation modes will be considered. Even further, field data could be used for training. Machine learning-based methods might directly predict the cavern capacity and even cavern shape in the field and serve as the next generation design tool for the construction of energy storage salt caverns.

Credit author statement

Li Jinlong: Conceptualization, Methodology, Software, Data curation, Writing – original draft, Writing – review & editing. **Zhuoteng Wang**: Data curation, Formal analysis, Visualization, Writing – original draft, **Shuai Zhang**: Software, Formal analysis, Writing – review & editing, **Xilin Shi**: Validation, Writing – review & editing, **Wenjie Xu**: Conceptualization, Writing – review & editing, **Duanyang Zhuang**: Writing – review & editing, **Jia Liu**: Writing – review & editing, **Qingdong Li**: Writing – review & editing, **Yunmin Chen**: Resources, Writing – review & editing.

Declaration of competing interest

The authors declare that they have no known competing financial interests or personal relationships that could have appeared to influence the work reported in this paper.

Acknowledgement

The authors wish to acknowledge the financial supports of National Natural Science Foundation of China (No. 52109138, 52122403), Basic Science Center Program for Multiphase Evolution in Hyper-gravity of the National Natural Science Foundation of China (No. 51988101), and Fundamental Research Funds for the Central Universities (No. 2021QNA4026). The authors are sincerely grateful to Jaak J Daemen, Mackay School of Earth Sciences and Engineering, University of Nevada, for his thoughtful review of this paper.

Appendix A. Supplementary data

Supplementary data to this article can be found online at https://doi.org/10.1016/j.energy.2022.124238.

References

[1] Aydin G. Production modeling in the oil and natural gas industry: an application of trend analysis. Petrol Sci Technol 2014;32:555–64. https://doi.org/10.1080/10916466.2013.825271.
[2] Yang C, Wang T, Li Y, Yang H, Li J, Qu D, et al. Feasibility analysis of using abandoned salt caverns for large-scale underground energy storage in China. Appl Energy 2015;137:467–81. https://doi.org/10.1016/j.apenergy.2014.07.048.
[3] Zhang N, Shi X, Zhang Y, Shan P. Tightness analysis of underground natural gas and oil storage caverns with limit pillar widths in bedded rock salt. IEEE Access 2020;8:12130–45. https://doi.org/10.1109/ACCESS.2020.2966006.
[4] Zhang N, Ma L, Wang M, Zhang Q, Li J, Fan P. Comprehensive risk evaluation of underground energy storage caverns in bedded rock salt. J Loss Prev Process Ind 2016:264–76. https://doi.org/10.1016/j.jlp.2016.10.016.
[5] International Gas Union. Report of working committee 2: underground gas storage. In: Proceedings of the 27th world gas conference; 2018. Washington.
[6] Aydin G, Karakurt I, Aydiner K. Analysis and mitigation opportunities of methane emissions from the energy sector. Energy Sources, Part A Recovery, Util Environ Eff 2012;34:967–82. https://doi.org/10.1080/15567031003716725.
[7] Ozarslan A. Large-scale hydrogen energy storage in salt caverns. Int J Hydrogen Energy 2012;37:14265–77. https://doi.org/10.1016/j.ijhydene.2012.07.111.
[8] Soubeyran A, Rouabhi A, Coquelet C. Thermodynamic analysis of carbon dioxide storage in salt caverns to improve the Power-to-Gas process. Appl Energy 2019;242:1090–107. https://doi.org/10.1016/j.apenergy.2019.03.102.
[9] Guo C, Pan L, Zhang K, Oldenburg CM, Li C, Li Y. Comparison of compressed air energy storage process in aquifers and caverns based on the Huntorf CAES plant. Appl Energy 2016;181:342–56. https://doi.org/10.1016/j.apenergy.2016.08.105.
[10] Li L, Liang W, Lian H, Yang J, Dusseault MB. Compressed air energy storage: characteristics, basic principles, and geological considerations. Adv Geo-Energy Res 2018;2(2):135–47. https://doi.org/10.26804/ager.2018.02.03.
[11] Li J, Xu W, Zheng J, Liu W, Shi X, Yang C. Modeling the mining of energy storage salt caverns using a structural dynamic mesh. Energy 2020;193:116730. https://doi.org/10.1016/j.energy.2019.116730.
[12] Cristescu ND, Paraschiv I. The optimal shape of rectangular-like caverns. Int J Rock Mech Min Sci Geomech Abstr 1995;32:285–300. https://doi.org/10.1016/0148-9062(95)00006-3.
[13] Li J, Shi X, Zhang S. Construction modeling and parameter optimization of multi-step horizontal energy storage salt caverns. Energy 2020;203:117840. https://doi.org/10.1016/j.energy.2020.117840.
[14] Steding S, Kempka T, Zirkler A. Spatial and temporal evolution of leaching zones within potash seams reproduced by reactive transport simulations. Water 2021;13:168. https://doi.org/10.3390/w13020168.
[15] Durie RW, Jessen FW. Mechanism of the dissolution of salt in the formation of underground salt cavities. Soc Petrol Eng J 1964;4:183–90. https://doi.org/10.2118/678-PA.
[16] Wanyan Q, Xiao Y, Tang N. Numerical simulation and experimental study on dissolving characteristics of layered salt rocks. Chin J Chem Eng: English version 2019;27:7. https://doi.org/10.1016/j.cjche.2019.01.004.
[17] Kazemi H, Jessen FW. Mechanism of flow and controlled dissolution of salt in solution mining. Soc Petrol Eng J 1964;4:317–28. https://doi.org/10.2118/1007-PA.
[18] Yang J, Li H, Yang C, Li Y, Han Y. Physical simulation of flow field and construction process of horizontal salt cavern for natural gas storage. J Nat Gas Sci Eng 2020:103527. https://doi.org/10.1016/j.jngse.2020.103527.
[19] Sears GF, Jessen FW. Controlled solution mining in massive salt. Soc Petrol Eng J 1966;6:115–25. https://doi.org/10.2118/1336-PA.
[20] Kunstman AS, Urbanczyk KM. UBRO - a computer model for designing salt cavern leaching process developed at CHEMKOP. Paris: Solution Mining Research Institute Fall Meeting; 1990.
[21] Saberian A, Von Schonfeldt. Convective mixing of water with brine around the periphery of vertical tube. Houston. In: Proceedings of the fourth symposium on salt; 1973.
[22] Liu W, Jiang D, Chen J, Daemen JJK, Tang K, Wu F. Comprehensive feasibility study of two-well-horizontal caverns for natural gas storage in thinly-bedded salt rocks in China. Energy 2018;143:1006–19. https://doi.org/10.1016/j.energy.2017.10.126.
[23] Liu W, Zhang Z, Chen J, Fan J, Jiang D, Daemen JJK, et al. Physical simulation of construction and control of two butted-well horizontal cavern energy storage using large molded rock salt specimens. Energy 2019;185:682–94. https://doi.org/10.1016/j.energy.2019.07.014.
[24] Sears GF, Jessen FW. Controlled solution mining in massive salt. Soc Petrol Eng J 1966;6:115–25. https://doi.org/10.2118/1336-PA.
[25] Saberian A. Numerical simulation of development of solution-mined storage cavities. Thesis Texas Univ; 1974.
[26] Nolen JS, Hantlemann O, Meister S, Kleinitz W, Heiblinger J. Numerical simulation of the solution mining process. SPE European Spring Meeting; 1974. https://doi.org/10.2118/4850-MS.
[27] Russo AJ. Solution mining code for studying axisymmetric salt cavern formation. Web: United States: N. p.; 1981. p. 1–40. https://www.osti.gov/biblio/5916427.
[28] Chaudan E. INVDIR: a convenient and efficient solution mining model. Paris: Solution Mining Research Institute Fall Meeting; 1990.
[29] Guarascio M. CAVITA: a multipurpose numerical code for brine production planning and cavern design and control. Solution Mining Research Institute Fall Meeting Cleveland; 1996. p. 375–404.
[30] Ban F. Study on optimization design of solution mining cavern for underground gas storage (in Chinese). University of Chinese Academy of Sciences; 2008.
[31] Li J, Shi X, Yang C, Li Y, Wang T, Ma H. Mathematical model of salt cavern leaching for gas storage in high-insoluble salt formations. Sci Rep 2018;8:372. https://doi.org/10.1038/s41598-017-18546-w.

[32] Li J, Yang C, Shi X, Xu W, Daemen J. Construction modeling and shape prediction of horizontal salt caverns for gas/oil storage in bedded salt. J Petrol Sci Eng 2020;190. https://doi.org/10.1016/j.petrol.2020.107058. 107058.
[33] Wan J, Peng T, Shen R, Jurado MJ. Numerical model and program development of TWH salt cavern construction for UGS. J Petrol Sci Eng 2019;179:930–40. https://doi.org/10.1016/j.petrol.2019.04.028.
[34] Ping X, Yang F, Zhang H, Zhang J, Zhang W, Song G. Introducing machine learning and hybrid algorithm for prediction and optimization of multistage centrifugal pump in an ORC system. Energy 2021;222:120007. https://doi.org/10.1016/j.energy.2021.120007.
[35] Cheng B, Du J, Yao Y. Machine learning methods to assist structure design and optimization of Dual Darrieus Wind Turbines. Energy 2022;244:122643. https://doi.org/10.1016/j.energy.2021.122643.
[36] Nair V, Hinton G. Rectified linear units improve restricted Boltzmann machines. In: Proceedings of the 27th international conference on machine learning. ICML-10); 2010. p. 807–14.
[37] Chollet, François. Keras: deep learning library for theano and tensorflow. 2015. https://github.com/fchollet/keras.
[38] Kingma D, Ba J. Adam: a method for stochastic optimization. International Conference on Learning Representations Meeting, San Diego, Canada. 2015. https://arxiv.org/abs/1412.6980.
[39] Nahler, Gerhard. Pearson correlation coefficient. Springer Vienna. 2009: 132–132. https://doi.org/10.1007/978-3-211-89836-9_1025.